

Direct observation of immiscibility in pyrope-almandine-grossular garnet

LIPING WANG,* ERIC J. ESSENE, AND YOUXUE ZHANG

Department of Geological Sciences, University of Michigan, Ann Arbor, Michigan 48109-1063, U.S.A.

ABSTRACT

Although recent thermodynamic models predict a low-temperature miscibility gap in the pyrope-almandine-grossular garnet solid-solution series, coexistence of two immiscible garnets consistent with the calculated miscibility gap has not been demonstrated previously. Here we report the discovery of such a coexistence in nature, which provides direct evidence for immiscibility in the pyrope-almandine-grossular system. Garnet inclusions were found near solidified fluid/melt inclusions in a single pyrope crystal collected from the ultramafic diatreme at Garnet Ridge, Arizona. Microprobe analyses close to the contact between the pyrope host and one garnet inclusion yield formulae of $(\text{Mg}_{1.98}\text{Ca}_{0.52}\text{Fe}_{0.50}\text{Mn}_{0.02})(\text{Al}_{1.89}\text{Cr}_{0.09})\text{Si}_3\text{O}_{12}$ for the host and $(\text{Mg}_{1.28}\text{Ca}_{1.31}\text{Fe}_{0.41}\text{Mn}_{0.02})(\text{Al}_{1.93}\text{Cr}_{0.07})\text{Si}_3\text{O}_{12}$ for the inclusion. High-resolution analytical traverses across the two-garnet boundary reveal that the compositional difference between the inclusion and the host increases as the contact is approached, implying that the two garnet grains represent an immiscible pair rather than a disequilibrium coexistence. The compositions of the coexisting garnets are in good agreement with those predicted from recent thermodynamic mixing models for pyrope-almandine-grossular garnet.

INTRODUCTION

Garnet is a common mineral in metamorphic and high-pressure igneous rocks and a major constituent of the Earth's mantle (e.g., Deer et al. 1982; Ringwood 1991). Its composition is generally dominated by a solid solution of three end-members: almandine ($\text{Fe}_3\text{Al}_2\text{Si}_3\text{O}_{12}$), grossular ($\text{Ca}_3\text{Al}_2\text{Si}_3\text{O}_{12}$), and pyrope ($\text{Mg}_3\text{Al}_2\text{Si}_3\text{O}_{12}$). Garnet plays a prominent role in quantitative geothermobarometric calculations to understand geological processes in the Earth (e.g., Essene 1989; Spear 1993). Reliable application of such calculations to natural rocks requires an understanding of the thermodynamic mixing properties of garnet solid solution. Although all recent mixing models imply immiscibility in the system at low temperatures (Berman and Aranovich 1996; Ganguly et al. 1996; Mukhopadhyay et al. 1997), and a ternary miscibility gap was calculated explicitly at $<600^\circ\text{C}$ (Ganguly et al. 1996), direct experimental verification of the predicted miscibility gap may not be possible because the kinetics of the exsolution process at such low temperatures are prohibitively slow. Thus, observation of an equilibrium coexistence of two garnets in natural assemblages would contribute direct evidence for immiscibility in garnet solid solutions. We report the discovery of such a coexistence, and use the analytical data to test recent thermodynamic models that predict immiscibility at low temperature.

SAMPLE AND ANALYTICAL METHODS

The sample, a single garnet megacryst (~6 mm in diameter) with a wine-red color, was collected from Garnet Ridge, Arizona, an ultramafic diatreme in the Navajo Volcanic Field on the Colorado Plateau. Similar garnet crystals are locally abundant in the diatreme and were brought up from the upper mantle by explosive eruption (e.g., McGetchin and Silver 1970; Hunter and Smith 1981). The initial examination of doubly polished thick sections (~3 mm thick) by an optical microscope revealed that the pyrope crystal (referred to as garnet host hereafter) contains mineral inclusions. The garnet host was repeatedly polished to bring individual inclusions to the surface and examined using back-scattered electron (BSE) imaging and an X-ray energy dispersive analytical system (EDS) on a Hitachi S-570 scanning electron microscope (SEM). Inclusions (10–60 μm across) with stoichiometric garnet compositions that are different from the garnet host were found during this process. The host and these inclusions were further characterized in detail by optical microscopy, Raman spectroscopy, SEM, and electron microprobe (EMP). The chemical analyses for the host and inclusions were carried out on a Cameca Camebax EMP using a focused beam with a current of 10 nA at 15 kV. Analytical traverses across inclusion-host boundaries were performed using a 1–3 μm interval and an acceleration voltage of 10 kV to reduce the beam volume. To improve the spatial resolution, step-scans for the $\text{CaK}\alpha$ line at a 0.5 μm interval were carried out on the SEM equipped with the VOYAGER application package (NORAN Instruments) using its EDS at 20 kV and 200 s counting time for each point. The diameter of the X-ray volume is less than 0.5 μm .

* Present address: Center for High Pressure Research and Department of Earth and Space Sciences, State University of New York at Stony Brook, Stony Brook, NY 11794-2100; E-mail: lipwang@notes.cc.sunysb.edu

RESULTS AND DISCUSSION

Garnet host

The garnet host contains inclusions of rutile, ilmenite, and olivine ($\sim\text{Fo}_{93}$). It also contains about 20 round composite inclusions comprised of carbonates (magnesite and dolomite), amphibole, Ba-K phlogopite, chlorapatite, and spinel. Such composite inclusions have been interpreted as solidified fluid/melt droplets (Smith 1987; Wang et al. 1999). Optical microscopic examination of thick sections of the garnet host showed that in three dimensions all inclusions are completely enclosed in the pyrope crystal, and in no case are they associated with cracks extending to the edge of the host. The host is chemically quite uniform (Mg:Fe:Ca \approx 67:18:15; Table 1), except for narrow diffusion halos around some included minerals such as olivine. The garnet also contains some Cr and minor levels of Mn and Ti. Based on the Cr content of this crystal and a systematic study on similar crystals from the same locality (Wang et al. 1999), we infer that it formed from the transition of spinel to garnet peridotite (i.e., spinel + pyroxene = garnet + olivine) at a pressure of \sim 20 kbar and a temperature between 600 and 650 °C in the presence of a fluid/melt phase. After it formed and equilibrated in a peridotitic assemblage, it experienced a long cooling history, as evidenced by the Mg-Fe diffusion profile in the garnet surrounding the olivine inclusion (Hunter and Smith 1981; Smith and Wilson 1985; Wang et al. 1999). The final temperature in the mantle before eruption is estimated to be $<$ 500 °C, based on the low content of Ca (0.7 wt% CaO) in magnesite coexisting with dolomite in the composite inclusions (e.g., Anovitz and Essene 1988).

Garnet inclusions

Three mineral inclusions that have a stoichiometric garnet composition were first found near two composite inclusions in

the garnet host (Fig. 1). Examination of 12 similar composite inclusions in the same host revealed only one additional such inclusion. All inclusions are found in contact with composite inclusions, but each inclusion is enclosed mainly by the garnet host. No such inclusion was observed in the host distant from the composite inclusions. BSE images clearly show: (1) the euhedral and approximately equidimensional shape of inclusions; (2) a sharp contact between inclusion and garnet host; and (3) a chemical difference between inclusion and host (Fig. 1). These observations suggest that they are two coexisting phases instead of simple heterogeneity or zoning.

One inclusion-host pair was examined with an optical microscope to see if there are optical differences between the inclusion and the garnet host. A thin section of the pair was prepared so that the inclusion was exposed on both polished surfaces. The sample is optically homogeneous. No differences in terms of appearance, color, relief, isotropy, reflective index, etc. can be discerned between the inclusion and the host. There is also no clear optical grain boundary for the inclusion (i.e., no outline of the inclusion, and no Becke line), suggesting that they have very similar refractive indices.

Raman spectra of the garnet host and an inclusion were taken to examine whether the inclusion is clearly of lower symmetry (i.e., deviation from a cubic symmetry, Deer et al. 1982). The micro-Raman spectrum of the inclusion has the same pattern as that of the garnet host and exhibits no peak splitting (Fig. 2). There is a small shift in peak positions, which is consistent with the demonstrated shift to high wavenumbers of Raman peaks with increasing Mg content of garnet (Moore et al. 1971). These results indicate that the inclusions examined have the same structure as the garnet host.

Representative EMP analyses of garnet inclusions and adjacent host are presented in Table 1. When compared to the garnet host, the garnet inclusions contain higher Ca and lower Mg. There

TABLE 1. Representative EMP analyses* of garnet host and garnet inclusion

| Oxides | H-1† | | H-2 | | H-3 | | H-4 | |
|---|-------|-------|-------|--------|-------|--------|-------|--------|
| SiO ₂ | 41.85 | 41.28 | 41.80 | 41.21 | 42.06 | 41.26 | 41.77 | 41.25 |
| TiO ₂ | 0.11 | 0.03 | 0.05 | 0.04 | 0.12 | 0.02 | 0.11 | 0.04 |
| Al ₂ O ₃ | 22.56 | 22.53 | 22.36 | 22.55 | 22.36 | 22.65 | 22.29 | 22.96 |
| Cr ₂ O ₃ | 1.58 | 1.14 | 1.63 | 1.14 | 1.72 | 0.86 | 1.59 | 0.55 |
| FeO‡ | 8.82 | 8.04 | 8.31 | 6.76 | 8.65 | 7.45 | 8.79 | 7.77 |
| MnO | 0.33 | 0.41 | 0.30 | 0.34 | 0.40 | 0.44 | 0.39 | 0.39 |
| MgO | 19.20 | 13.51 | 18.54 | 11.85 | 19.36 | 11.87 | 19.33 | 13.01 |
| CaO | 5.27 | 13.02 | 6.76 | 16.89 | 5.25 | 15.95 | 5.30 | 14.45 |
| Total | 99.72 | 99.96 | 99.75 | 100.78 | 99.92 | 100.50 | 99.57 | 100.42 |
| Formula proportions based on eight cations | | | | | | | | |
| Si | 2.998 | 3.004 | 2.997 | 2.986 | 3.006 | 3.000 | 2.996 | 2.987 |
| Ti | 0.006 | 0.002 | 0.003 | 0.002 | 0.006 | 0.001 | 0.006 | 0.002 |
| Al | 1.904 | 1.933 | 1.890 | 1.926 | 1.884 | 1.941 | 1.884 | 1.960 |
| Cr | 0.089 | 0.066 | 0.092 | 0.065 | 0.097 | 0.049 | 0.090 | 0.031 |
| Fe | 0.528 | 0.489 | 0.498 | 0.410 | 0.517 | 0.453 | 0.527 | 0.471 |
| Mn | 0.020 | 0.025 | 0.018 | 0.021 | 0.024 | 0.027 | 0.024 | 0.024 |
| Mg | 2.050 | 1.466 | 1.982 | 1.280 | 2.063 | 1.286 | 2.066 | 1.404 |
| Ca | 0.404 | 1.015 | 0.519 | 1.311 | 0.402 | 1.242 | 0.407 | 1.121 |
| Prp§ | 67.3 | 47.6 | 64.4 | 40.7 | 67.6 | 41.7 | 67.4 | 46.0 |
| Gr§ | 14.2 | 35.4 | 18.2 | 45.2 | 14.2 | 42.7 | 14.2 | 38.0 |
| Alm | 18.5 | 17.0 | 17.4 | 14.1 | 18.2 | 15.6 | 18.4 | 16.0 |

* The compositions are expressed as oxide weight percent.

† H-1: garnet host and garnet inclusion pair No. 1. In each pair, the left column is for the host, and the right column is for the inclusion.

‡ All Fe as FeO.

§ The end-member proportions are calculated by first subtracting the khorringite ($\text{Mg}_3\text{Cr}_2\text{Si}_3\text{O}_{12}$) component from the formulae, then normalizing among Ca, Fe, and Mg. Mn and Ti are ignored.

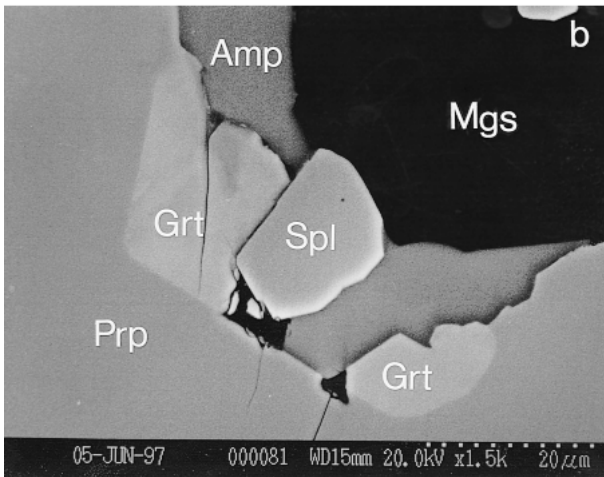
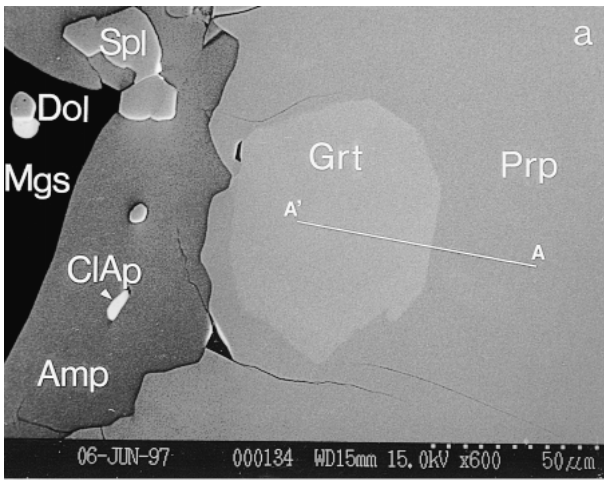


FIGURE 1. BSE images showing natural coexistence of two garnets. Abbreviations: Amp = amphibole; ClAp = chlorapatite; Dol = dolomite; Grt = garnet inclusion; Mgs = magnesite; Prp = garnet host; Spl = spinel. Amphibole, chlorapatite, dolomite, magnesite, and spinel are mineral constituents of composite inclusions, which are inferred to be solidified droplets of fluid/melt. Line AA' in (a) is the locus of EMP traverse shown in Figure 3a.

is also a noticeable decrease in the content of Cr, Fe, and Ti and a small increase in Mn in garnet inclusions (Table 1). Three microprobe traverses across inclusion-host boundaries were made and one is shown in Figure 3a. The traverse (1–3 μm interval) reveals slight zoning in the garnet inclusion, whereas the garnet host near the inclusion is quite uniform (Fig. 3a). The contact between the garnet inclusion and the host is sharp. Other traverses show similar features.

Host and inclusion: stable immiscible pair or disequilibrium coexistence?

Equilibrium between coexisting phases is difficult, often impossible, to demonstrate unequivocally. Here we establish a method to distinguish a stable immiscible pair from simple dis-

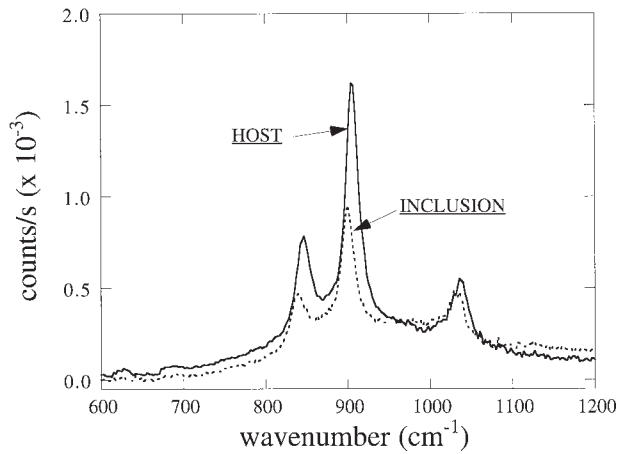


FIGURE 2. Raman spectra of garnet host and garnet inclusion collected using non-polarized laser beam with a wavelength of 532.4 nm.

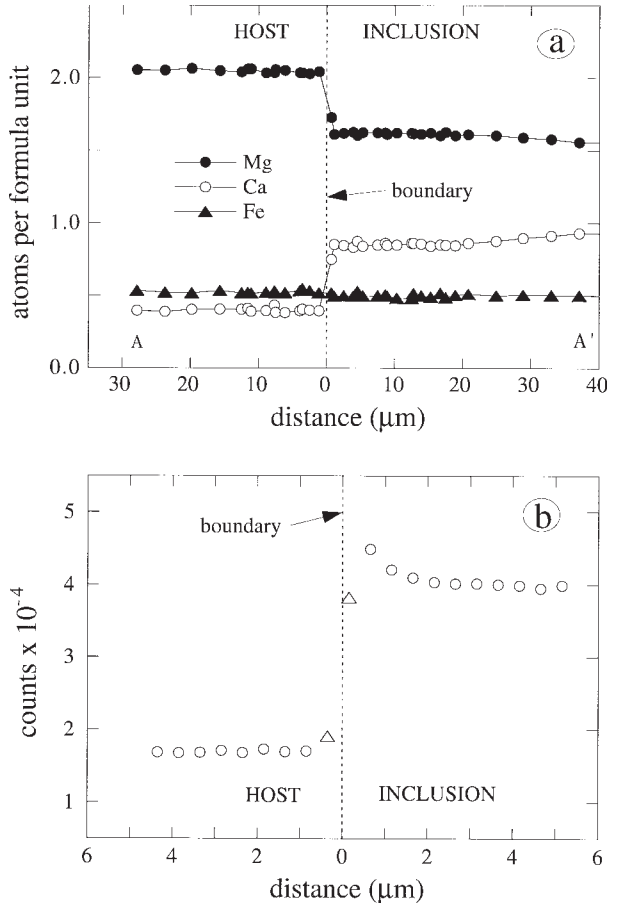


FIGURE 3. Analytical traverses across the contact between garnet host and garnet inclusion. (a) Concentration profiles for Mg, Ca, and Fe from EMP analysis. The intermediate values of Mg and Ca at the boundary represent beam overlap of the two garnet compositions. (b) Concentration profile for Ca from EDS analysis on SEM. The points close to the boundary (shown as open triangles) are affected by the convolution effect. The counting errors of both EMP and SEM analyses are smaller than the size of symbols.

equilibrium coexistence. Consider a schematic phase diagram of a solid solution series with a miscibility gap at low temperatures (Fig. 4a). If two grains form immiscible phases at equilibrium, then as the system cools, the miscibility gap widens, leading to a greater compositional difference across the boundary of the two grains (solid curves in Fig. 4b). If two grains simply represent the disequilibrium coexistence of two compositionally different crystals in a single phase field, they will tend to homogenize by diffusion, leading to a continuous concentration profile (dashed curve in Fig. 4b). The length over which the concentration varies (either widening or bridging the compositional gap) is twice

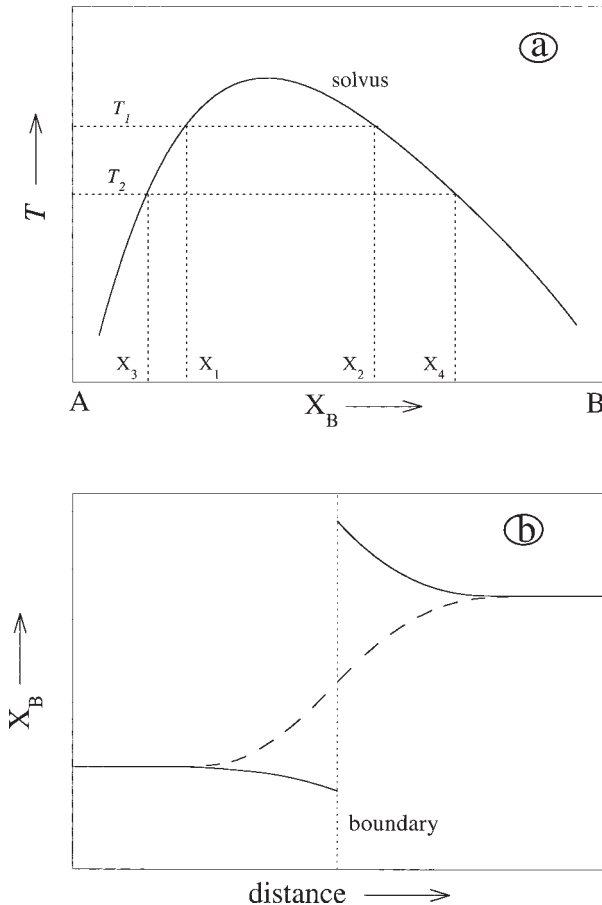


FIGURE 4. (a) A schematic phase diagram of a binary solution series (A and B) with an asymmetric miscibility gap at low temperatures (T). The compositional difference between two equilibrium phases across the miscibility gap increases ($X_4 - X_3 > X_2 - X_1$) upon cooling ($T_2 < T_1$). Note the compositional change upon cooling for the phase on the B-side solvus limb ($X_4 - X_3$) is greater than that for the phase on the A-side solvus limb ($X_2 - X_1$). (b) A schematic drawing showing how an immiscible pair responds to cooling differently from that of two disequilibrium coexisting grains in a single phase field. The horizontal profile in both grains represents the initial composition. Solid curve: for an immiscible pair; the compositional gap widens across the boundary upon cooling. Note different amounts of compositional change for the pair at the boundary. Dashed curve: for two disequilibrium grains in a single phase field; they tend to homogenize upon cooling.

the square root of $\int Ddt$ where D is the diffusivity (and hence dependent on temperature) and t is the duration.

The measured electron microprobe profile (Fig. 3a) does not have sufficient spatial resolution to distinguish whether the Ca concentration difference between the two garnet grains increases or decreases as the boundary is approached. Although very high spatial resolution can be achieved by a transmission electron microscope (TEM), sample preparation is extremely difficult due to the small size and the rarity of garnet inclusions (one sample was lost during such an attempt). Analysis using EDS on the SEM was found to have a much better spatial resolution than the EMP and was used to examine further the garnet inclusion-host contact. Step-scans across the boundary were carried out using the $\text{CaK}\alpha$ line at a $0.5 \mu\text{m}$ interval with a beam volume of $\leq 0.5 \mu\text{m}$ across and 200 s counting time for each point. The beam current remained stable during the course of analysis, as evidenced by the uniform concentration in the interior of the garnet inclusion and that of the garnet host (Fig. 3b). The results show that, in the garnet host, there is no clear trend except for a slight increase in Ca very close to the boundary owing to the convolution effect (Ganguly et al. 1988). The absence of a clear decrease in Ca concentration in the host as the contact is approached is a consequence of the steepness of the T - X slope of the Ca-poor limb of the solvus (Ganguly et al. 1996) and mimics that in the case of Fe-Ni exsolution (Wood 1964). However, there is clearly an increase of Ca in the garnet inclusion toward the contact (Fig. 3b). This trend must be real since analytical artifacts such as convolution effect would narrow, not widen, the Ca concentration gap. Therefore, the compositional gap between the garnet inclusion and the host widened upon cooling, demonstrating that the two garnet grains represent an immiscible pair rather than a simple disequilibrium coexistence.

Origin of immiscible host-inclusion pairs

An *exsolution* origin for immiscible garnet pairs is not supported by the analytical microprobe traverses (i.e., no significant zonation in garnet host; Fig. 3a) and the inferred low temperature for the host formation (i.e., too large a diffusion distance required). Overgrowth of the host garnet megacryst on the inclusion garnet is unlikely because (1) garnet inclusions are always in contact with composite inclusions and (2) they are not observed in many similar garnet megacrysts from the same locality (McGetchin and Silver 1970; Hunter and Smith 1981; Smith 1987; Wang et al. 1999). The close association of all garnet inclusions with composite inclusions (which are inferred to be fluid/melt inclusions before solidification; Smith 1987; Wang et al. 1999) suggests that the formation of the garnet inclusion was related to the evolution of fluid/melt inclusions (i.e., growth of garnet host or inclusion from included fluid/melt). The following is a possible although speculative scenario. At higher temperatures, the fluid/melt inclusions were in equilibrium with the host garnet. As temperature decreased, two different garnet compositions (across the miscibility gap) were in equilibrium with the fluid/melt. Therefore, either or both of the two immiscible garnets could precipitate. Precipitation of garnet with a composition close to that of the host (i.e., continuous formation of the host) would form layers that are indistinguishable from the early crystallized host. Precipitation of garnet with a composition

across the miscibility gap (i.e., composition of the inclusion garnet) would form garnet inclusions. The rarity of garnet inclusions suggests that the continuous growth of the garnet host was favored probably because no interface formation was required. The tendency to minimize interfacial energy (hence interfacial area) may explain the roughly euhedral shape for the garnet inclusions instead of lamellae or coronae over the host, which is commonly observed for disequilibrium overgrowths on metamorphic garnet (e.g., Spear 1993). The co-precipitation of both garnets from included fluid/melt can explain the observation that each garnet inclusion is enclosed mainly by garnet host. In this interpretation, the surrounding pyrope near garnet inclusions would be continuous growth layers that cannot be distinguished from the early host.

Testing thermodynamic models

Because Cr and Mn contents are low, both the garnet host and inclusions are approximated by the pyrope-almandine-grossular system. The miscibility gap in this system has been calculated using three thermodynamic mixing models for garnet (Berman and Aranovich 1996; Ganguly et al. 1996; Mukhopadhyay et al. 1997). The pressure effect is insignificant in the range of 0–30 kbar based on these models, and a pressure of 20 kbar, the estimated pressure for the garnet host, was chosen in our calculations. The isotherms calculated from all three models predict similar solvi for the garnets. For clarity, only solvi from the model of Ganguly et al. (1996), along with EMP analyses for four inclusion-host pairs several micrometers away from their contacts, are shown in Figure 5. All the data lie between the 400 and 450 °C isotherms. They lie between 430–480 °C for the Berman and Aranovich (1996) model and 370–420 °C for the Mukhopadhyay et al. (1997) model. Furthermore, the Fe content does not change significantly from garnet host to garnet inclusion in both observation and calculation. Considering that these solvi are calculated by large extrapolation and that the effect of Cr and Mn on phase equilibria is neglected, the agreement between our data and the thermodynamic models is remarkable. However, the compositions of garnet inclusions among different grains have a larger range in Ca/Mg ratio than predicted from the models (i.e., Fig. 9a in Ganguly et al. 1996), suggesting that the solvus limb on the pyrope side may be steeper and that on the grossular side may be flatter than predicted by the models. Whether the temperatures obtained above are accurate depends on the accuracy of the mixing models and whether minor Cr and Mn affect the mixing properties significantly.

Previous reports of immiscibility in pyrope-almandine-grossular garnet

Exsolution inferred from a TEM study of a grossular-almandine-pyrope garnet from a metarodingite sample has been reported before in an abstract (Ghose et al. 1976), but no chemical analyses were given for the coexisting garnets. One of the co-authors of the abstract, B.W. Evans, kindly provided such a metarodingite sample (no. Mg-31-I). Using BSE imaging and EMP analysis, we found complex zoning instead of exsolution in garnets, and we hence conclude that the suite of garnets reported by Ghose et al. (1976) is unlikely to represent an equilibrium assemblage or an immiscible pair.

Cressey (1978) observed under TEM what appear to be two immiscible garnet phases (polyhedral garnet inclusions of 0.1–0.4 μm across with $X_{\text{Grs}} \approx 0.2$ in a garnet matrix with $X_{\text{Grs}} \approx 0.36$) in an apparently optically homogeneous garnet (bulk $X_{\text{Grs}} = 0.29$, $X_{\text{Alm}} = 0.49$) from a granulite. No detailed compositions were reported for the two phases. His observation provides the best previous evidence of a possible miscibility gap for pyrope-almandine-grossular garnet. However, if it indeed represents a solvus, then the immiscibility occurs in almandine-rich garnet ($X_{\text{Alm}} = 0.49$), whereas recent thermodynamic models (Berman and Aranovich 1996; Ganguly et al. 1996; Mukhopadhyay et al. 1997) predict, and our observations confirm, that the immiscibility occurs in almandine-poor garnet ($X_{\text{Alm}} = 0.14\text{--}0.19$ in our sample) at temperatures between ~ 400 and ~ 600 °C. The incoherence of the Ca-enriched included phase relative to the garnet host (Cressey 1978; Cressey et al. 1978) suggests that the two phases may have different structures.

Yardley et al. (1996) observed complicated two-phase intergrowths in pyrope-poor and almandine-rich garnet ($X_{\text{Prp}} = 0.02\text{--}0.04$ and $X_{\text{Alm}} = 0.54\text{--}0.75$) overgrowing pyrope-rich relicts. The authors considered a number of possible mechanisms (including equilibrium coexistence across a miscibility gap) for the origin of the intergrowths but noted that no explanation is entirely convincing. The presence of pyrope-rich relicts and the pyrope-poor composition suggest that the intergrowths are unlikely to represent equilibrium immiscible pairs.

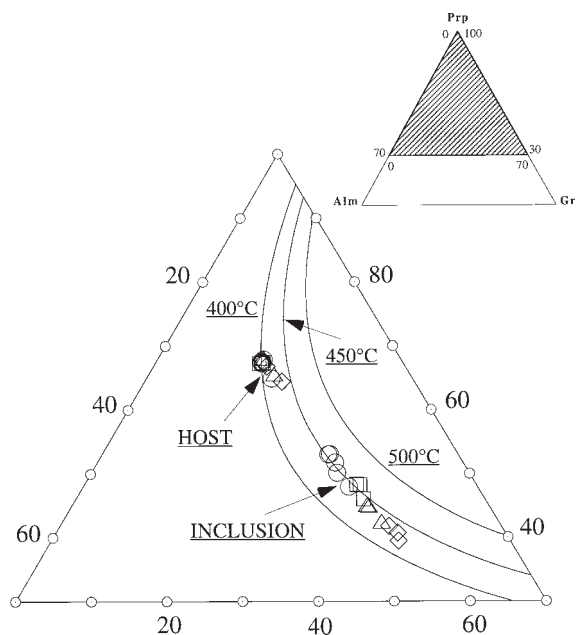


FIGURE 5. Calculated miscibility gap from one of the recent mixing models for garnet (Ganguly et al. 1996). The diagram shown is the shaded area in the pyrope-almandine-grossular ternary system. The data are EMP analyses done for host-inclusion pair several micrometers away from their contact (i.e., Table 1). Different symbols represent different host-inclusion pairs: circles = pair 1; diamonds = pair 2; triangles = pair 3; and squares = pair 4. The errors from EMP analyses are less than the size of the symbols.

CONCLUDING REMARKS

The discovery presented here represents the best evidence for immiscibility in the pyrope-almandine-grossular system. This study not only demonstrates that two immiscible garnets can coexist in nature in equilibrium, hence providing a critical constraint for the thermodynamic mixing properties of garnet, but also establishes a method for distinguishing immiscible pairs from disequilibrium coexistence. Moreover, it confirms a relatively low temperature in the upper mantle beneath the Four Corners area of the Colorado Plateau at the time of eruption of ultramafic diatremes, consonant with many previous studies (e.g., Helmstaedt and Doig 1975; Hunter and Smith 1981; Smith and Wilson 1985; Smith 1995; Wang et al. 1999).

ACKNOWLEDGMENTS

This paper grew out of a seminar run by Y. Zhang in 1997. In addition to the authors, other participants in the seminar included S. Keane, Y. Liu, W. Yu, D. Zhao, among others. We thank S. Dunn, S.C. Semken, and A. Zaman for their help in field work, the Navajo Nation for permission to collect samples, N.L. Jester for taking the Raman spectra, and B.W. Evans for providing the metaroddingite sample (no. Mg-31-I). Comments from J. Ganguly, D.M. Jenkins, A.M. Koziol, D.R. Peacor, D. Smith, and two anonymous reviewers greatly improved the presentation. This study was partially supported by grants from NSF (EAR 93-15918, 94-58368, 95-26596, and 97-25566), the Department of Indian Affairs and Northern Development, Canada, the University of Michigan, and the Geological Society of America.

REFERENCES CITED

- Anovitz, L.M. and Essene, E.J. (1988) Phase equilibria in the system $\text{CaCO}_3\text{-MgCO}_3\text{-FeCO}_3$. *Journal of Petrology*, 28, 389–414.
- Berman, R.G. and Aranovich, L.Ya. (1996) Optimized standard state and solution properties of minerals: I. model calibration for olivine, orthopyroxene, cordierite, garnet, and ilmenite in the system $\text{FeO-MgO-CaO-Al}_2\text{O}_3\text{-TiO}_2\text{-SiO}_2$. *Contributions to Mineralogy and Petrology*, 126, 1–24.
- Cressey, G. (1978) Exsolution in almandine-pyrope-grossular garnet. *Nature*, 271, 533–534.
- Cressey, G., Schmid, R., and Wood, B.J. (1978) Thermodynamic properties of almandine-grossular garnet solid solutions. *Contributions to Mineralogy and Petrology*, 67, 397–404.
- Deer, W.A., Howie, R.A., and Zussman, J. (1982) *Rock-Forming Minerals: Orthosilicates*. Second Edition, Vol. 1A, 919 p. Wiley, New York.
- Essene, E.J. (1989) The current status of thermobarometry in metamorphic rocks. In J.S. Daly, R.A. Cliff, and B.W.D. Yardley, Eds., *Evolution of Metamorphic Belts*, p. 1–44. Geological Society Special Publication 43.
- Ganguly, J., Bhattacharya, R.N., and Chakraborty, S. (1988) Convolution effect in the determination of compositional profiles and diffusion coefficients by microprobe step scans. *American Mineralogist*, 73, 901–909.
- Ganguly, J., Cheng, W., and Tirone, M. (1996) Thermodynamics of aluminosilicate garnet solid solution: new experimental data, an optimized model, and thermometric applications. *Contributions to Mineralogy and Petrology*, 126, 137–151.
- Ghose, S., Leo, S.R., and Evans, B.W. (1976) Exsolution in a grossular-almandine-pyrope garnet. Program with Abstracts of Geological Association of Canada and Mineralogical Association of Canada, p. 80.
- Helmstaedt, H. and Doig, R. (1975) Eclogite nodules from kimberlite pipes of the Colorado Plateau—samples of subducted Franciscan-type oceanic lithosphere. *Physics and Chemistry of the Earth*, 9, 95–111.
- Hunter, W.C. and Smith, D. (1981) Garnet peridotite from Colorado Plateau ultramafic diatremes: hydrates, carbonates, and comparative geothermometry. *Contributions to Mineralogy and Petrology*, 76, 312–320.
- McGetchin, T.R. and Silver, L.T. (1970) Compositional relations in minerals from kimberlite and related rocks in the Moses Rock dike, San Juan County, Utah. *American Mineralogist*, 55, 1738–1771.
- Moore, R.K., White, W.W., and Long, T.V. (1971) Vibrational spectra of the common silicates: I. the garnets. *American Mineralogist*, 56, 54–71.
- Mukhopadhyay, B., Holdaway, M.J., and Koziol, A.M. (1997) A statistical model of thermodynamic mixing properties of Ca-Mg-Fe²⁺ garnets. *American Mineralogist*, 82, 165–181.
- Ringwood, A.E. (1991) Phase transformations and their bearing on the constitution and dynamics of the mantle. *Geochimica et Cosmochimica Acta*, 55, 2083–2110.
- Smith, D. (1987) Genesis of carbonate in pyrope from ultramafic diatremes on the Colorado Plateau, southwestern United States. *Contributions to Mineralogy and Petrology*, 97, 389–396.
- (1995) Chlorite-rich ultramafic reaction zones in Colorado Plateau xenoliths: recorders of sub-Moho hydration. *Contributions to Mineralogy and Petrology*, 121, 185–200.
- Smith, D. and Wilson, C.R. (1985) Garnet-olivine equilibration during cooling in the mantle. *American Mineralogist*, 70, 30–39.
- Spear, F.S. (1993) *Metamorphic Phase Equilibria and Pressure-Temperature-Time Paths*. Mineralogical Society of America Monograph, 799 p.
- Wang, L., Essene, E.J., and Zhang, Y. (1999) Mineral inclusions in pyrope crystals from Garnet Ridge, Arizona, USA: implications for processes in the upper mantle. *Contributions to Mineralogy and Petrology*, 135, 164–178.
- Wood, J.A. (1964) Cooling rates of iron meteorites. *Icarus*, 3, 429–459.
- Yardley, B.W.D., Condliffe, E., Lloyd, G.E., and Harris, D.H.M. (1996) Polyphase garnets from west Ireland: two-phase intergrowths in the grossular-almandine series. *European Journal of Mineralogy*, 8, 383–392.

MANUSCRIPT RECEIVED FEBRUARY 17, 1999

MANUSCRIPT ACCEPTED AUGUST 8, 1999

PAPER HANDLED BY DAVID M. JENKINS